DOI: 10.1002/chem.200601753

Effects of Chain Length and N-Methylation on a Cation–π Interaction in a β-Hairpin Peptide

Robert M. Hughes, Matthew L. Benshoff, and Marcey L. Waters*[a]

Abstract: The effects of N-methylation and chain length on a cation–π interaction have been investigated within the context of a β-hairpin peptide. Significant enhancement of the interaction and structural stabilization of the hairpin have been observed upon Lys methylation. Thermodynamic analysis indicates an increased entropic driving force for folding upon methylation of Lys residues. Comparison of lysine to analogues ornithine (Orn) and diaminobutyric acid (Dab) indicates that lysine provides the strongest cation–π interaction and also provides the most stable β-hairpin due to a combination of side chain–side chain interactions and β-sheet propensities. These studies have significance for the recognition of methylated lysine in histone proteins.

Keywords: amino acids · cation–pi interactions · noncovalent interactions · peptides · protein models

Introduction

The role of the cation–π interaction between a cationic residue (lysine or arginine) and an aromatic residue (tryptophan, tyrosine, or phenylalanine) in proteins is a topic of continuing interest due to its relevance to protein structure,[1] the mediation of protein–protein interactions,[2] and protein–ligand interactions.[1] These interactions have been observed in statistical analyses of protein structures[1] and even in de novo designed proteins.[3] Post-translational modifications of cationic residues in proteins play important roles in cellular processes through the mediation of protein–protein interactions. One example of this phenomenon is lysine methylation in histone proteins, in which the methylation of lysine results in binding to an aromatic pocket of chromodomain proteins, thus modulating the process of chromatin condensation.[4] In general, the binding of small molecules containing quaternary ammonium ions in protein binding pockets lined with aromatic residues, such as the binding of acetylcholine to acetylcholine esterase, is a well known event in structural biology and has been utilized in seminal studies of molecular recognition.[5]

[a] R. M. Hughes, M. L. Benshoff, Dr. M. L. Waters
Department of Chemistry
University of North Carolina at Chapel Hill
Chapel Hill, NC 27599–3290 (USA)
Fax: (+1) 919-962-2388
E-mail: mlwaters@email.unc.edu

Supporting information for this article is available on the WWW under http://www.chemeurj.org/ or from the author.

In a previous study, we have shown that the trimethylation of lysine significantly increases the magnitude of the cation–π interaction between a lysine and a tryptophan residue in the context of a well-folded β-hairpin peptide.[6] Our current study has two aims: 1) to systematically explore both the effect of mono, di, and trimethylation of lysine on the magnitude of the interaction and 2) to study the influence of the proximity of the methylated ammonium group to tryptophan with the lysine (Lys) analogues ornithine (Orn) and diaminobutyric acid (Dab), in which the alkyl chain is shortened by one and two methylenes, respectively (Figure 1). By incrementally methylating the Orn and Dab side chains in the same manner as Lys, we investigated the optimal length for interaction of the unmethylated cationic side chain with tryptophan and determined whether the same chain length was still optimal upon methylation. As a result, this study allows us to investigate the maximal interaction energy of the cation-π interaction within our model system. Additionally, this study reveals the interplay between the contributions of side chain–side chain interactions and β-sheet propensity to overall β-hairpin stability. Both β-sheet propensity, which is the statistical preference for a particular amino acid to adopt a β-sheet conformation, and side chain–side chain interactions have been shown to contribute to β-hairpin stability.[7] In this study, we find that while β-sheet propensity decreases in the order Lys > Orn > Dab, the magnitude of the cation–π interaction between the truncated cationic residues and Trp still increases with N-methylation, lending stability to the hairpin and offsetting much of the destabilizing effects of low β-sheet propensity.

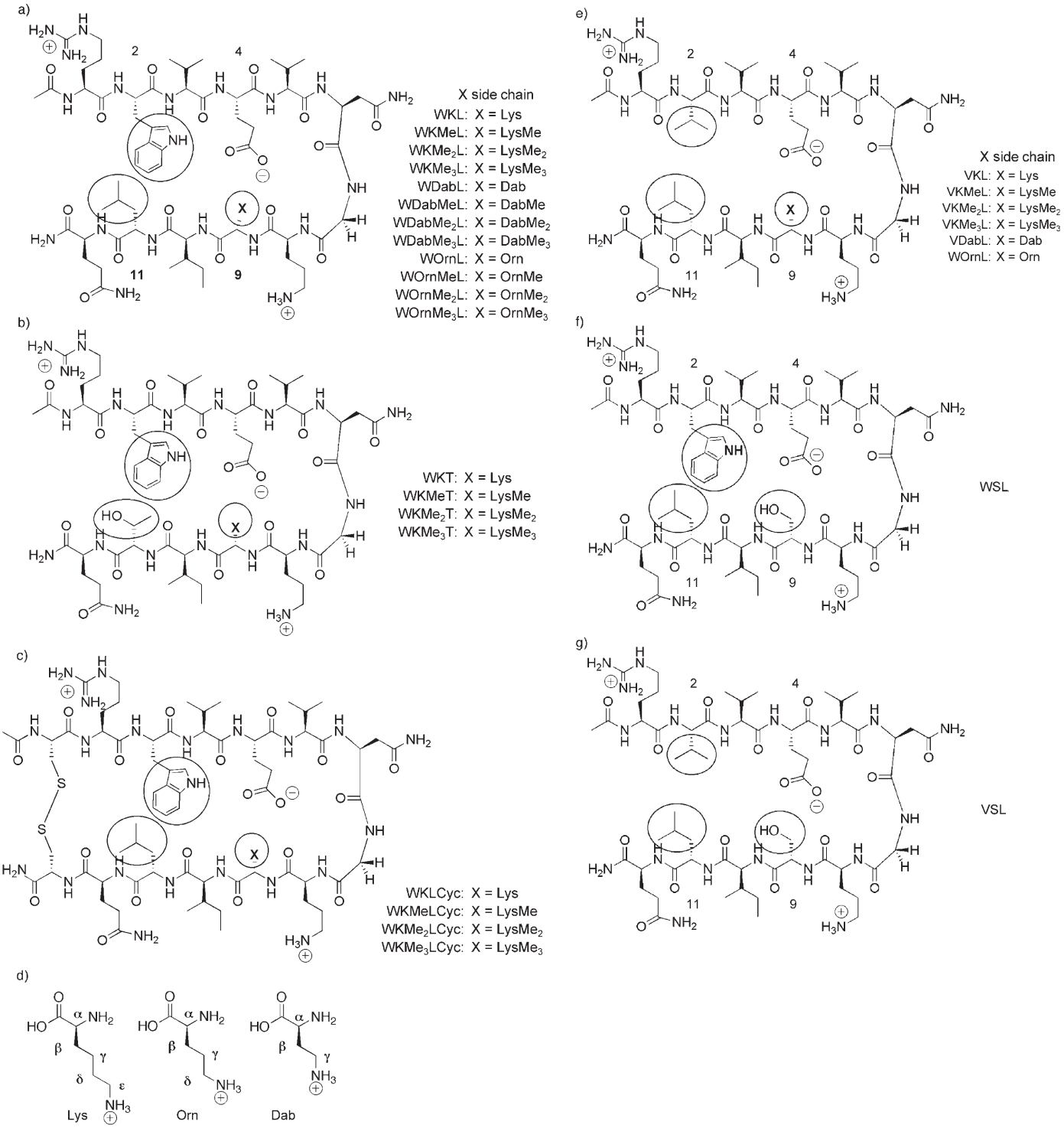

Figure 1. a) β-Hairpin peptides WXL, containing Lys, Orn, and Dab at position 9, and their methylated analogues. b) β-Hairpin peptides WXT, containing Lys and its methylated analogues at position 9, with Leu 11 mutated to Thr. c) Cyclic peptides WXLcyc are disulfide bridged at the hairpin termini to represent the fully folded state. The 7 mers (not shown) are used to determine the random coil chemical shifts (see the Supporting Information). d) Structure of Lys, Orn, and Dab. e) Single mutant peptides VXL, in which Trp 2 has been replaced with Val. f) Single mutant peptide WSL in which residue X at position 9 has been replaced with Ser. g) Double mutant peptide VSL in which Trp 2 has been replaced by Val and residue X at position 9 has been replaced with Ser.

Results and Discussion

Design, synthesis, and characterization: Peptides were designed to exploit a known energetically favorable cation–π interaction between Lys and Trp in diagonally oriented non-hydrogen-bonded positions on the same face of the β-hairpin (Figure 1).[8] Due to the right-handed twist of the hairpin fold, the cross strand diagonal positions 2 (Trp) and 9 (Lys)

place their respective side chains in closer proximity than the diagonal positions 4 (Glu) and 11 (Leu).[7] This creates a favorable environment for the side chains to interact if an attractive force exists between them. We initially studied peptides with Leu at position 11, laterally cross-strand from Trp 2 (Figure 1a). Due to the very high stability of the original Leu-containing peptide series (and therefore small differences in fraction folded, which result in large differences in ΔG when near fully folded) Leu was mutated to Thr to create a less stable series of β-hairpins (Figure 1b), such that variation in hairpin stability could be measured more accurately.

Methylated amino acids were synthesized as shown in Schemes 1 and 2. Monomethylated species were synthesized starting with either Boc-Orn-OH (**1a**; Boc = *tert*-butoxycarbonyl) or Boc-Dab-OH (**1b**) (Scheme 1). Following protection of the side chain with *o*-nitrobenzene sulfonic acid, amino acid **2** was selectively methylated in the presence of NaOH with dimethyl sulfate. Deprotection of **3** with TFA (TFA = trifluoroacetic acid) and reprotection with Fmoc-Cl (Fmoc = 9-fluorenylmethyloxycarbonyl) gave **4**. After solid-phase peptide synthesis, the *o*-nitrobenzenesulfonyl moiety was selectively cleaved in the presence of 2-mercaptoethanol and DBU (DBU = 1,8-diazabicyclo[5.4.0]undec-7-ene),[9] followed by cleavage from the resin with TFA. Boc-dimethyl Orn (**6a**) and Boc-dimethyl Dab (**6b**) were prepared from Boc-Orn (**1a**) and Boc-Dab (**1b**) by reductive methylation in the presence of formaldehyde and H_2/Pd/C (Scheme 2).[10] The Boc-protected amino acids were deprotected with TFA, reprotected with Fmoc-OSu, and incorporated into peptides by means of standard Fmoc solid-phase peptide synthesis. Trimethylated species were achieved by methylation of dimethyllysine with methyl iodide and MTBD (MTBD = 7-methyl-1,5,7-triazabicyclo[4.4.0]dec-5-ene) after peptide synthesis, followed by cleavage from the resin.[11]

Peptides were characterized by mass spectrometry and NMR spectroscopy as reported previously.[8] Alpha hydrogen (H_α) chemical shifts, glycine splitting, and NOEs were used to characterize the hairpin structure and their respective stabilities. The degree of H_α chemical shifts of the hairpins relative to random coil values (Figure 1c–d) are used as indicators of the degree of β-sheet structure at each position along the strand.[12] In the folded state, H_α are shifted downfield relative to random coil due to the inductive effects of the amide-carbonyl cross-strand hydrogen bonds present in β-sheets.[13] Hence, increased downfield H_α shifting is evidence of increased hairpin stability. Also, the magnitude of glycine splitting has been shown to be a good indicator of overall hairpin stability.[14] The extent of folding can be quantified by calculating the fraction folded, as shown by the following equation: fraction folded $(f) = [\delta_{obs} - \delta_0]/[\delta_{100} - \delta_0]$, in which δ_0 represents the random coil chemical shift determined from 7 mer peptides and δ_{100}, the fully folded chemical shift determined from the cyclic peptides (Figure 1). Free energy of folding is determined from the fraction folded value by the equation $\Delta G = -RT\ln(f/(1-f))$.

Side chain chemical shifts were used to evaluate the proximity of the cationic side chain to the Trp indole ring. Due to the anisotropy of the aromatic ring, protons that are in close proximity to the electron-rich face of an aromatic ring are shifted upfield. As a result, the degree of Lys side-chain upfield shifting is an indicator of the degree of contact between the alkyl side chain and the face of the tryptophan ring. Finally, NOEs between cross-strand pairs of side chains provide evidence for hairpin folding within the correct register. These are provided in the Supporting Information.

Effects of chain length in unmethylated side chains: Comparison of WKL, WOrnL, and WDabL allows for the influ-

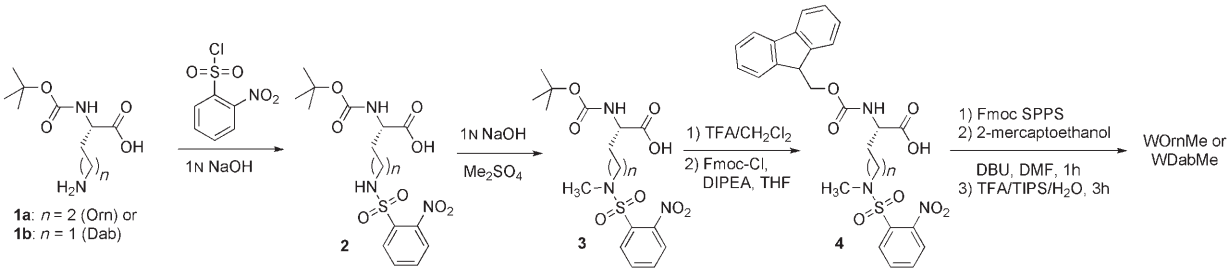

Scheme 1. Synthesis of monomethylated Orn and Dab-containing peptides.

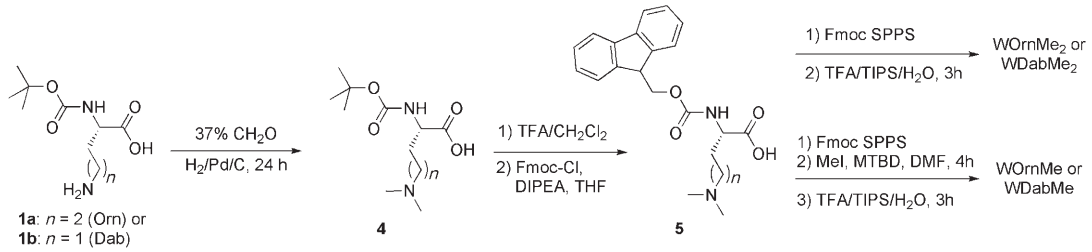

Scheme 2. Synthesis of di- and trimethylated Orn and Dab-containing peptides.

ence of the chain length on the cation–π interaction to be determined. To correct for differences in β-sheet propensities of Dab, Orn, and Lys double mutant cycles were performed,[15] indicating that the cation–π interactions for WKL and WOrnL are −0.3 and −0.2 (±0.1) kcal mol^{-1}, respectively. Due to the instability of the Dab single mutant hairpin VDabL (fraction folded = 13%), large errors in the double mutant cycles complicate a direct analysis of the contribution of the side chain–Trp interaction to hairpin stability for WDabL. However, based on the trends in upfield shifting of the Lys, Orn, and Dab side chains (Figure 2), the

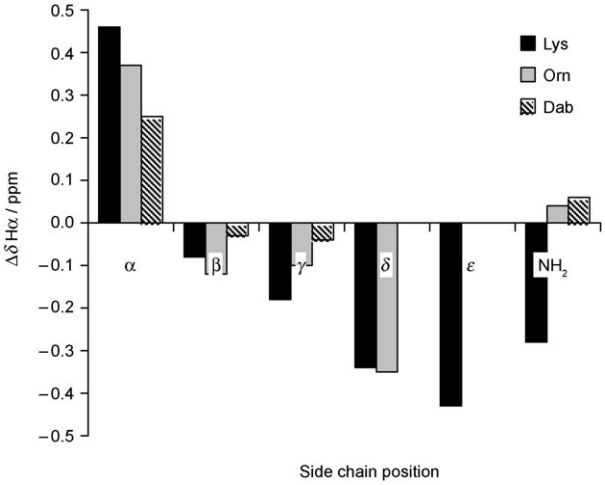

Figure 2. Upfield shifts of Lys, Orn, and Dab side chains.

available evidence suggests that the cation-π component of the side-chain-Trp interaction decreases with each truncation of the side chain. Indeed, for Dab it appears that there is little or no interaction with Trp, as the upfield shifting is <0.05 ppm at any position in the Dab side chain (Figure 2). This suggests that Dab is too short to interact with Trp in a diagonal orientation. The upfield shifting of Orn suggests that the δ-position is the most favorable for interaction with Trp, but that it is not as favorable as the ε-position of Lys. Hence, Lys appears to be of the optimal length for a diagonal cation–π interaction.

The fraction folded of the control peptides, VKL, VOrnL, and VDabL, in which a cation–π interaction is not possible, provides information about the inherent β-sheet propensity of Orn and Dab relative to Lys. As the side chain is shortened, its β-sheet propensity decreases, resulting in a decreased fraction folded (from 37% for VKL to 29% for VOrnL to 13% for VDabL). Hence, mutation of Lys to Orn and Dab results in destabilization of the β-hairpin due to the reduced β-sheet propensity even in the absence of a cation–π interaction. Additionally, the fraction folded of the single mutant peptides does not change significantly upon methylation (for example, VKL (37%) and VKMe$_3$L (38%)). This indicates that in the case of the WX(Me)$_n$L peptides (where X = Lys, Orn or Dab and n = 0–3), it is indeed enhancement of the side chain–side chain interaction by means of methylation, and not a change in β-sheet propensity upon methylation, that lends added stability to the peptide (see discussions of methylated peptides below).

Effects of lysine methylation: peptides WK(Me)$_n$L (n = 0–3): The lysine-containing peptides WKL, WKMeL, WKMe$_2$L, and WKMe$_3$L show an increase in hairpin stability with each addition of a methyl group to the lysine side chain, revealing that even monomethylation significantly stabilizes the folded peptide (Table 1 and Figure 3a). This trend is also

Table 1. Fraction folded and stability of hairpins at 298 K.

Peptide	% Folded (Gly)[a]	% Folded (H$_\alpha$)[b]	ΔG [kcal mol^{-1}][c]
WKL	78 (1)	76 (10)	−0.76 (−0.7)
WKMeL	86 (1)	84 (13)	−1.06 (−1.0)
WKMe$_2$L	89 (1)	84 (16)	−1.26 (−1.0)
WKMe$_3$L	92 (1)	91 (15)	−1.45 (−1.4)

[a] Error is ±1% as determined from the error in chemical shift. [b] Percent folded from H$_\alpha$ shifts is the average of the values from residues 2–5 and 8–11, excluding the turn residues and the termini. The standard deviation is in parenthesis. [c] Determined from the Gly splitting; values in parentheses are from the H$_\alpha$ data. Error is ±0.05 kcal mol^{-1}, as determined from the error in the chemical shift; Average error for H$_\alpha$ data (as calculated from the standard deviation) is ±0.4 kcal mol^{-1}.

evident in the H$_\alpha$ shifts, which are further downfield upon methylation, with the exception of the frayed terminal residues arginine and glutamine, which are not significantly affected by methylation, and Asn in the β turn (Figure 3b).

The lysine side chain also exhibits increased upfield shifting with each additional methylation, indicating a greater degree of interaction with the tryptophan indole ring (Figure 3c). The ε methylene is the most upfield-shifted portion of the side chain in each peptide, indicating its close proximity to the indole ring. In the case of Lys, the ε protons are polarized by the neighboring cationic ammonium group, which creates a site of favorable interaction with the face of the aromatic ring. This is consistent with the orientation of Lys–Trp pairs commonly observed in protein crystal structures (Figure 4).[16]

To quantitatively assess the Lys–Trp interaction, double mutant cycles were performed, by using the noninteracting residues Ser and Val in place of Trp and Lys, respectively (Figure 1).[8] Double mutant cycles isolate the interaction energy of the residues in question (in this case, Lys and Trp), and extracts the contribution of this interaction to the overall ΔG of hairpin folding. The single mutant peptides (Trp2Ser and Lys9Val) account for the contribution of each residue in the interacting pair (Trp or Lys) to β-hairpin stability, while the double mutant peptide accounts for changes in stability that may be due to differences in β-sheet propensities etc. between the native and mutant side chains. Double mutant cycles provide Lys–Trp interaction energies for WKL, WKMeL, WKMe$_2$L, and WKMe$_3$L of −0.3, −0.5, −0.7, and −1.0 kcal mol^{-1} (±0.1 kcal mol^{-1}), respectively. This amounts to an enhancement of the cation–π interaction of about 0.2–0.3 kcal mol^{-1} per methylation. The value of

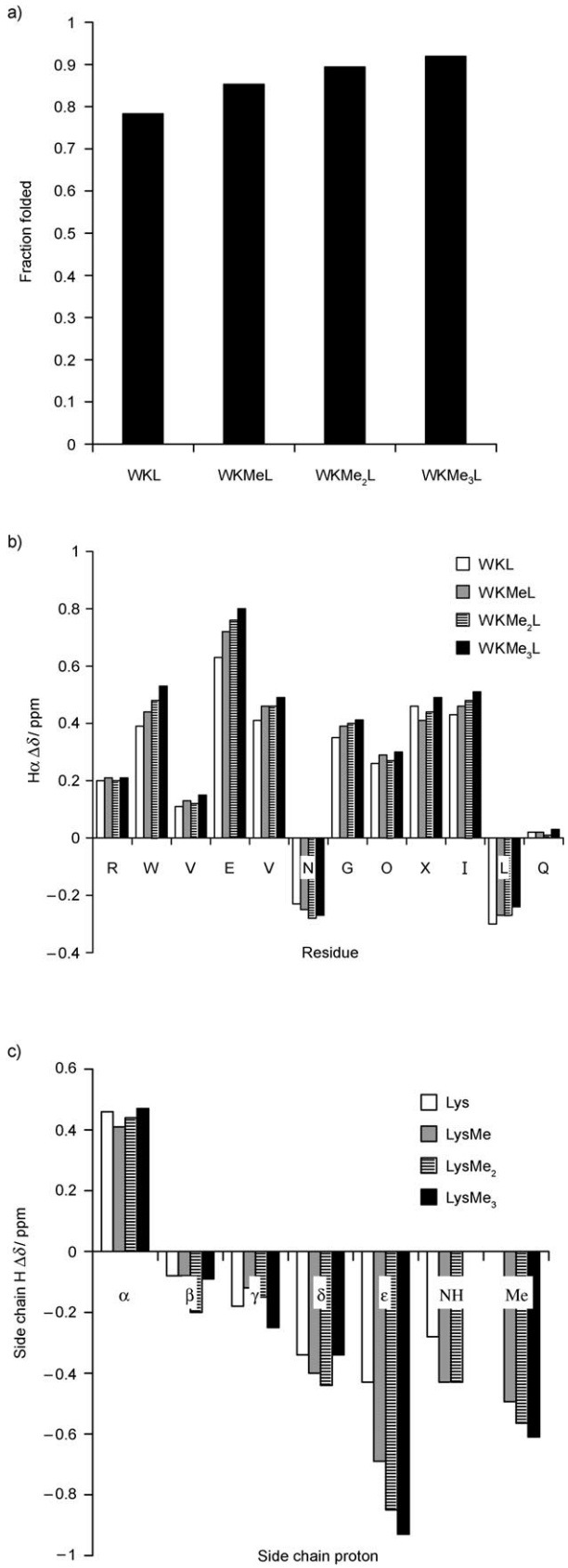

Figure 3. a) Fraction folded derived from the glycine splitting. b) WK(Me)$_n$L H_α shifts relative to random coil values. Glycine shifts reflect the splitting. c) WK(Me)$_n$L side chain upfield proton shifts relative to random coil values.

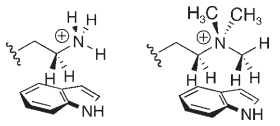

Figure 4. Possible interaction geometries for Trp–Lys and Trp–KMe$_3$ interactions.

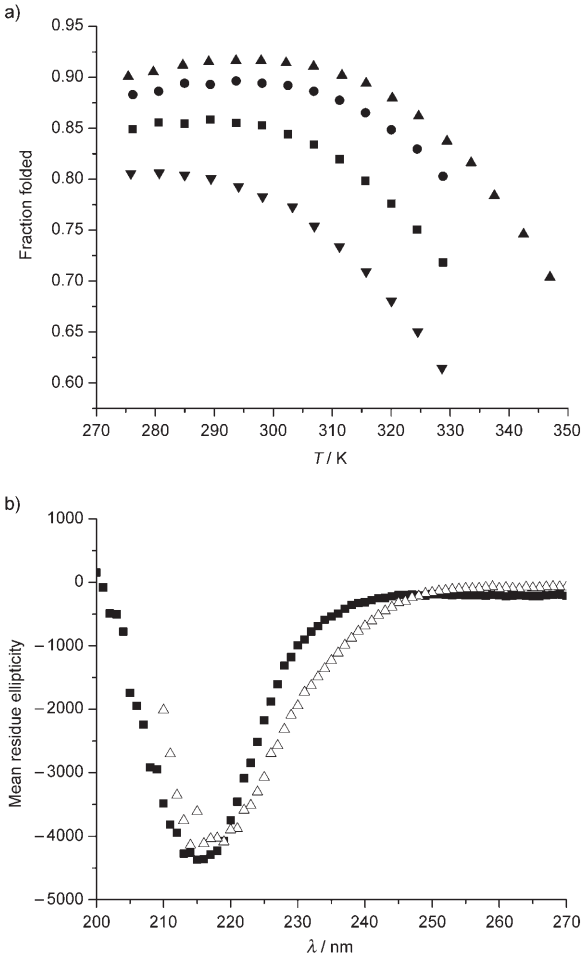

Figure 5. a) Thermal denaturation profiles of WK(Me)$_n$L peptides by NMR spectroscopy. ▼: WKL, ■: WKMeL, ●: WKMe$_2$L, ▲: WKMe$_3$L. b) CD spectra of WKMe$_3$L at 0 (■) and 90°C (△).

−1.0 kcal mol^{-1} for the interaction of trimethylated lysine with tryptophan compares well with other literature values for the binding of tetra-alkyl ammonium species to aromatic rings in water: approximately 0.9 kcal mol^{-1} per aromatic residue in Diederich's study of a Factor Xa binder,[5a] and approximately 1.1 kcal mol^{-1} per aromatic residue in Dougherty's cyclophane receptor.[17b]

The methylated hairpins WKMeL, WKMe$_2$L, and WKMe$_3$L show a significant increase in thermal stability in comparison to the parent peptide WKL (Figure 5a). By NMR spectroscopic analysis, WKMe$_3$L appears to be ≈72% folded at 70°C. Interestingly, the trimethylated peptide WKMe$_3$L shows little or no thermal denaturation by CD over the range 0 to 90°C (Figure 5b). The peptide WKMe$_3$L

also shows no unfolding transition over the 20 to 90 °C range when monitored by DSC. These results corroborate a recent FTIR study of the thermal denaturation of the β-hairpin peptide trpzip2, which maintains substantial residual native structure when heated to 82 °C.[18] Taken together, these results support the notion that the global β-sheet structure of $WKMe_3L$ changes little over a wide temperature range, making it impractical to measure a thermal transition with traditional calorimetry techniques, such as DSC. The CD spectrum gives insight into the global stability of the hairpin, while the NMR spectrum can reveal detailed structural changes indistinguishable by CD. Notable exceptions to this are the trpzip peptides, which display large exciton couplings, enabling accurate determination of thermodynamic parameters from thermal CD studies.[19]

Analysis of the thermodynamics of folding derived from NMR thermal denaturation reveals increasingly favorable entropy of folding and increasingly unfavorable enthalpy of folding with each methylation step (Table 2). The decrease in enthalpic favorability can be explained by the greater dispersion of the positive charge across the N-methyl groups in KMe_3, as can be seen from the electrostatic potential maps in Figure 6. The increase in entropic favorability is consistent with additional sites of interaction with the aromatic ring with each additional methyl group: while the lysine side chain in hairpin WKL has one preferred site of interaction (the polarized ε methylene), the methylated peptides WKMeL, $WKMe_2L$, and $WKMe_3L$ have additional polarized methyl groups that can interact favorably with the aromatic ring. In addition, the enhanced hydrophobicity of the side chain upon methylation is also reflected by the trend in ΔS. There is also a trend of increasingly favorable ΔC_p° with each methylation, which is usually associated with an increased hydrophobic effect and may be the result of increased burial of the lysine side chain with each methylation.[20]

Table 2. Thermodynamic parameters[a] for $WK(Me)_nL$ ($n=0$–3) peptides at 298 K.[10]

Peptide	$\Delta H°$ [kcal mol^{-1}]	$\Delta S°$ [cal mol^{-1} K^{-1}]	ΔC_p° [cal mol^{-1} K^{-1}]
WKL	−2.8 (0.03)	−6.8 (0.1)	−163 (3)
WKMeL	−1.7 (0.1)	−2.2 (0.3)	−221 (33)
$WKMe_2L$	−0.7 (0.1)	+1.8 (0.4)	−207 (31)
$WKMe_3L$	−0.1 (0.1)	+4.5 (0.3)	−243 (36)

[a] Determined from the temperature dependence of the Gly chemical shift from 0 to 60 °C for peptide WKL, WKMeL, and $WKMe_2L$ and from 0 to 80 °C for the peptide $WKMe_3L$. Conditions: 50 mM [D_4]sodium acetate, pH 4.0 (uncorrected) at 298 K, referenced to DSS. Errors (in parentheses) are determined from the fit.

$WK(Me)_nT$ ($n=0$–3) peptides: Because the series of methylated $WK(Me)_nL$ peptides are so well folded (near 100%), we had some concern about the accuracy of the ΔG values, which had been determined from the fraction folded. This is because small changes in the fraction folded result in larger changes in ΔG when the peptide is near 100% folded than when it is near 50% folded. Hence, we reinvestigated the Trp-$Lys(Me)_n$ interactions by using a peptide series in which the fraction folded of the peptide containing unmethylated Lys was only modestly folded. In addition to the cation–π interaction, another stabilizing structural feature of this family of β-hairpins is the hydrophobic packing of the Trp residue with the cross-strand Leu. This interaction stabilizes the hydrophobic core of the folded peptide, as demonstrated by a series of lysine-containing peptides in which Leu is mutated to Thr (Figure 1b), leading to a less well-folded family of β-hairpins (Figure 7). Thr has been observed to have a lower β-sheet propensity than Leu in other β-hairpin model systems.[22] It is also clear from the chemical shifts of the Thr and Leu side chains from $WK(Me)_nT$ and $WK(Me)_nL$ peptides that Thr does not interact with Trp as strongly as does Leu (Figure 8). Hence, the observed destabilization of the

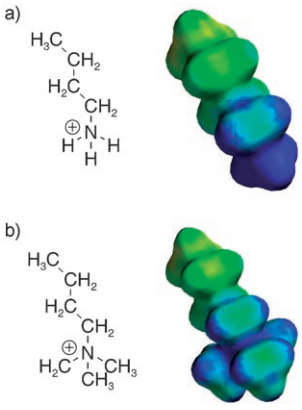

Figure 6. Electrostatic potential maps of a) a lysine side chain analogue and b) trimethylated lysine side chain analogue (Spartan: HF/6–31 g*; scale = 50 to 200 kcal mol^{-1}).[21] Chemdraw structures are included to show the orientation of the side chain.

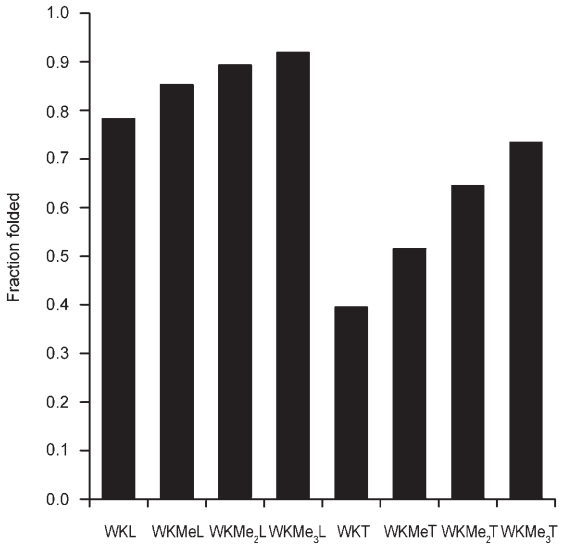

Figure 7. Fraction folded (based on glycine splitting) of $WK(Me)_nT$ and $WK(Me)_nL$ ($n=0$–3) β-hairpins.

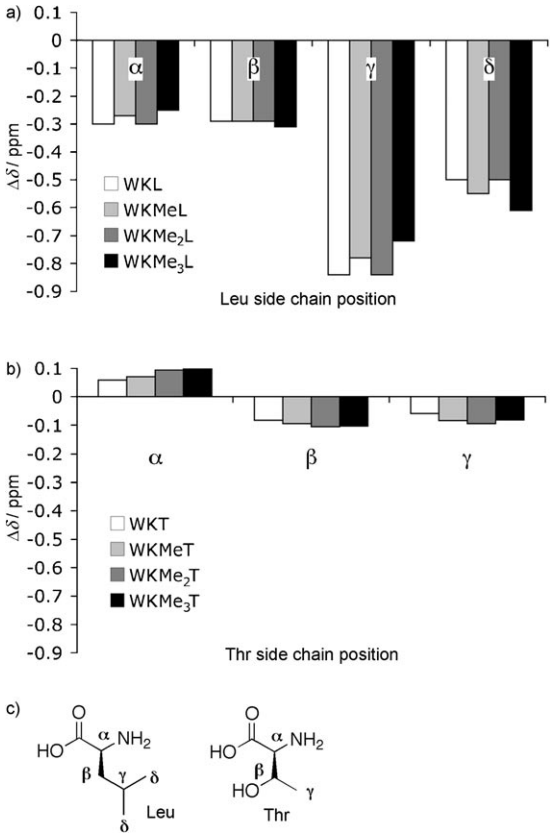

Figure 8. a) Upfield shifts of Leu in WK(Me)$_n$L peptides (n=0–3). b) Upfield shifts of Leu in WK(Me)$_n$T peptides (n=0–3). c) Structures of Leu and Thr with side chain positions labeled.

hairpin appears to be a combination of side chain–side chain interactions and β-sheet propensity effects.

Comparison of hairpin stabilities from the WK(Me)$_n$L series of peptides and the WK(Me)$_n$T series indicate that the differences in energy upon each methylation are within error in the two series (Table 3). This indicates that the values determined from the WK(Me)$_n$L series are reliable, and hence, the double mutant data discussed above for the WK(Me)$_n$L series is correct. Moreover, this demonstrates the modular nature of these systems for studying noncovalent interactions, in that two different peptide systems provide the same information on cation–π interactions.

Table 3. Comparison of hairpin stabilities in the WKL and WKT series.

Peptide	Fraction folded	$\Delta G°$ [kcal mol^{-1}]	$\Delta\Delta G$[a] [kcal mol^{-1}]
WKL	0.78	−0.76	–
WKMeL	0.85	−1.04	−0.28
WKMe$_2$L	0.89	−1.26	−0.22
WKMe$_3$L	0.92	−1.44	−0.18
WKT	0.39	0.27	–
WKMeT	0.50	−0.01	−0.27
WKMe$_2$T	0.63	−0.32	−0.31
WKMe$_3$T	0.73	−0.58	−0.26

[a] $\Delta\Delta G° = \Delta G°(\text{WK(Me)}_n\text{X}) - \Delta G°(\text{WK(Me)}_{n-1}\text{X})$, for which n=0–3 and X=Leu or Thr.

WOrn(Me)$_n$L peptides (n=0–3): From the ornithine-containing peptide series (WOrnL, WOrnMeL, WOrnMe$_2$L, WOrnMe$_3$L), it is apparent that shortening the length of the side chain by one methylene destabilizes the folded peptide (Figure 9a). The $\Delta G°$ of folding for WKL is −0.77 kcal mol^{-1}, while the $\Delta G°$ of WOrnL is −0.42 kcal mol^{-1}. As seen with the lysine series, hairpin stability increases with each methylation of Orn, so that the stability of the trimethylated Orn hairpin WOrnMe$_3$L is approximately that of the unmethylated lysine hairpin WKL (Figure 9b). As compared to the methylated lysine series, the methylated Orn side chains show similar trends in their upfield shifting relative to

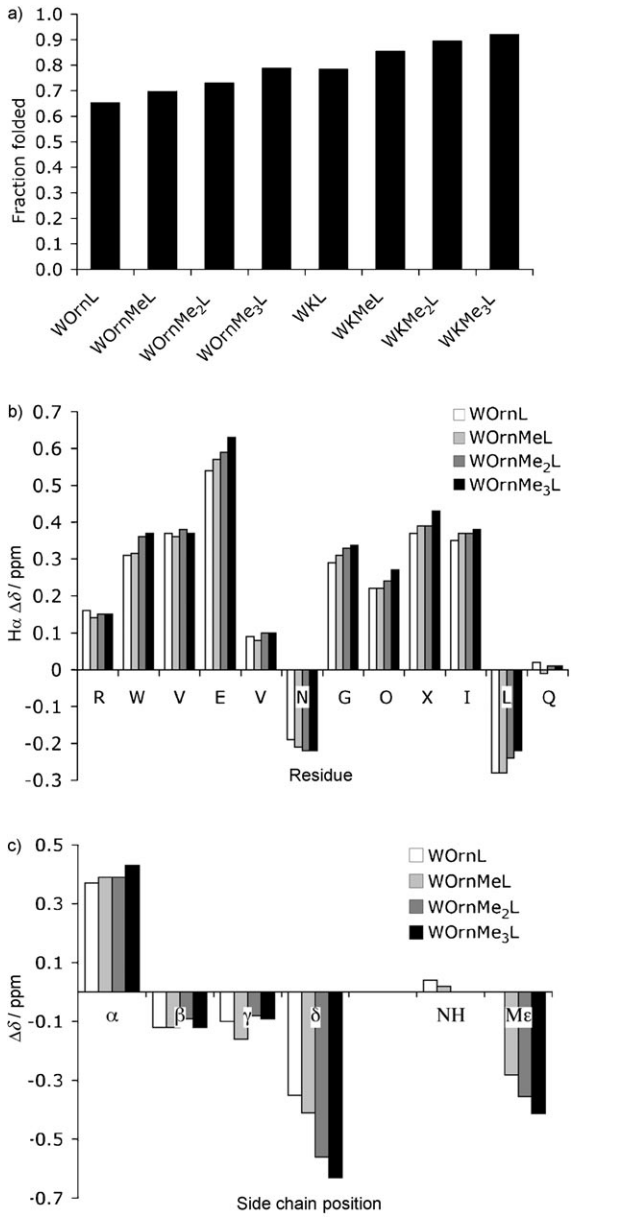

Figure 9. a) WOrn(Me)$_n$L and WK(Me)$_n$L fraction folded from the glycine splitting. b) WOrn(Me)$_n$L H$_\alpha$ shifts relative to random coil values. Glycine shifts reflect the splitting. c) WOrn(Me)$_n$L side chain upfield proton shifts relative to random coil values.

random coil due to their proximity to the aromatic ring (Figure 9c). However, with ornithine the polarized δ-position is the most upfield shifted portion of the side chain, indicating that it is the preferred side of interaction with the indole ring. This is directly analogous to the Lys–Trp interaction, in which the methylene adjacent to the ammonium group is the preferred site of interaction with Trp. As seen in the methylated lysines, the N-terminal methyl groups are significantly upfield shifted, but less so than the δ protons (Figure 9c).

Double mutant cycles performed for the peptides WOrnL and $WOrnMe_3L$ show that methylation of the Orn side chain lends added stability to the Trp–Orn interaction, just as in the case of the Lys–Trp interaction, with the cation–π interaction worth $-0.2\,kcal\,mol^{-1}$ in WOrnL and $-0.8\,kcal\,mol^{-1}$ in $WOrnMe_3L$ ($\pm 0.1\,kcal\,mol^{-1}$). The fact that the cation–π interaction is worth slightly less in the Orn peptides versus the Lys peptides is born out by the upfield shifting profiles, which show less upfield shifting for the Orn side chains than for the Lys side chains (Figure 10).

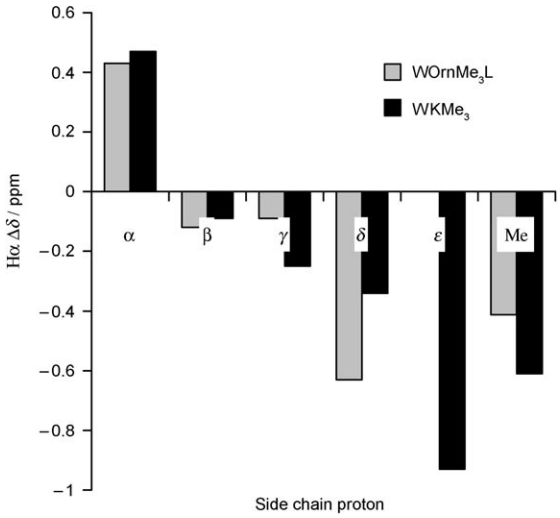

Figure 10. Comparison of $OrnMe_3$ and $LysMe_3$ side chain upfield shifting profiles.

WDab(Me)$_n$L Peptides (n = 0–3): In the diaminobutyric acid (Dab)-containing peptides (WDabL, WDabMeL, $WDabMe_2L$, and $WDabMe_3L$), the trends in global hairpin stability observed for the methylation of Lys and Orn continue (Figure 11a): Dab is less stable than Orn or Lys. This is evident from both the fraction folded derived from the glycine splitting and the H_α downfield shifts (Figure 11b). However, due to the shortened side chain of Dab, the preferred site of interaction with Trp changes in comparison to Orn and Lys. While there is some upfield shifting along the Dab side chain (Figure 11c), the magnitude of the methylene shifts proximal to the cation is minor compared to those observed for both the Lys and Orn peptides (-0.95 ppm for the ε methylene of $WKMe_3L$ and -0.72 ppm for the δ methylene of $WOrnMe_3L$ versus -0.1 ppm for the γ methylene of

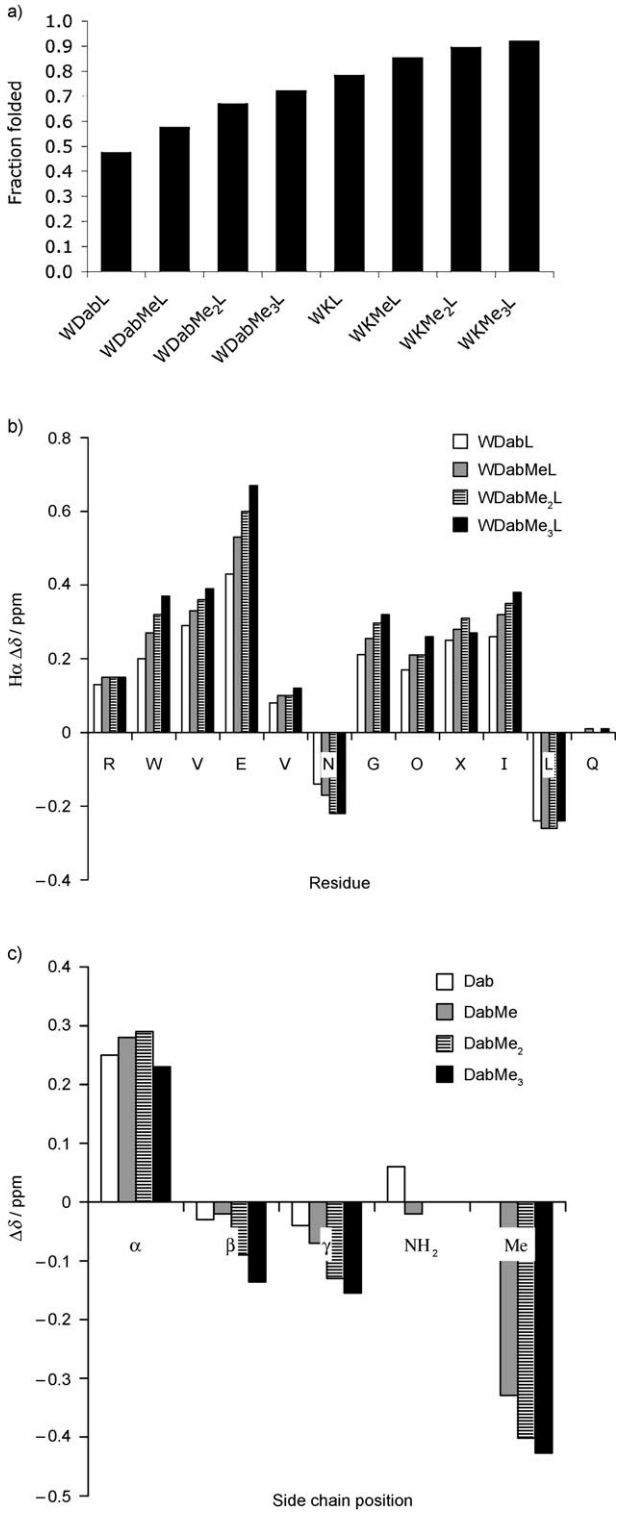

Figure 11. a) WDab(Me)$_n$L and WK(Me)$_n$L fraction folded comparison. b) WDab(Me)$_n$L H_α shifts relative to random coil values. Glycine shifts reflect the splitting. c) WDab(Me)$_n$L side chain upfield proton shifts relative to random coil values.

$WDabMe_3L$). Additionally, while the N-methyl groups of Orn(Me)$_n$ and Lys(Me)$_n$ are less upfield shifted than their δ and ε methylenes, respectively (Orn: $\delta = -0.4$ versus

−0.7 ppm; Lys: $\delta = -0.6$ versus −1.0 ppm), the Dab(Me)$_n$ methyl groups are by far the most upfield-shifted portion of the Dab side chain (−0.4 ppm). The Dab N-methyl groups are at the same location as the Lys ε methylene. Thus, it appears that due to length restriction, the Dab N-terminal methyl groups are the only portion of the side chain to experience significant contact with the indole ring. Double mutant cycles for the Trp–Dab interaction possess higher error (0.2 kcal mol^{-1}) due to the instability of the Trp to Val single mutant peptides in the Dab series (fraction folded ≈14%). Thus, they give numbers that are within error for those of the Orn and Lys peptides ($\Delta\Delta G = -0.3$ kcal mol^{-1} for the Trp–Dab interaction in WDabL and $\Delta\Delta G = -0.9$ kcal mol^{-1} for the Trp–DabMe$_3$ interaction in WDabMe$_3$L, all values ±0.2 kcal mol^{-1}). Nonetheless, the magnitude of the Trp-DabMe$_3$ interaction, despite the decreased upfield shifting relative to LysMe$_3$ and OrnMe$_3$ side chains, suggests that it may be able to interact with the Trp side chain in a nonspecific, hydrophobic fashion (for example, packing against the side of the ring) in addition to undergoing a cation–π interaction with the face of the indole ring via its N-terminal methyl groups. Additionally, given the similarity of the interaction magnitudes of the cationic residues with Trp, the trends in overall hairpin stability suggest that the Dab residues also have lower β-sheet propensities than their Orn and Lys analogues.

pH studies: It is conceivable that the shortening of the lysine side chain to diaminobutyric acid might actually favor the formation of a salt bridge with the cross strand glutamic acid (Figure 1a). We have previously demonstrated the effect of protonating the Glu in WKL by showing that lowering the pH increases hairpin stability.[8] Consistent with our initial observations, all peptides in the series show an increase in stability upon lowering the pH, which is consistent with hydrophobic packing of the alkyl chains of Lys, Orn, and Dab with the alkyl group of the Glu side chain, rather than the formation of a traditional salt bridge (Figure 12). Furthermore, mutation of Glu to Gln eliminates the pH dependence of stability. Similar hydrophobic interactions between lysine and glutamic acid have been observed in related coiled-coil systems.[23,24]

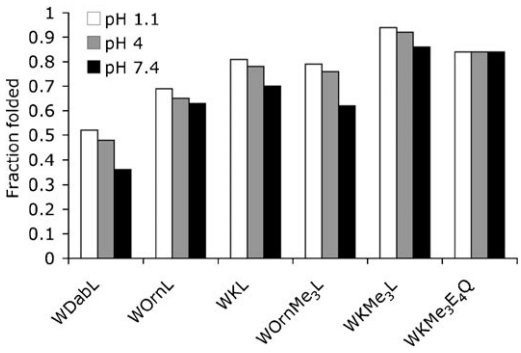

Figure 12. pH study of hairpin stability (based on glycine splitting).

NMR structure calculation: The calculation of NMR solution structures was undertaken to further confirm our experimental observations. By using the program CNSSolve, a simulated annealing protocol was used in conjuction with NMR chemical shift and NOE data to generate a number of low-energy structures for the β-hairpins WKL and WKMe$_3$L.[25] Shown below are selected 10 lowest-energy structures from the simulated annealing runs (Figure 13). The superimposed backbone structures show the hydrogen-

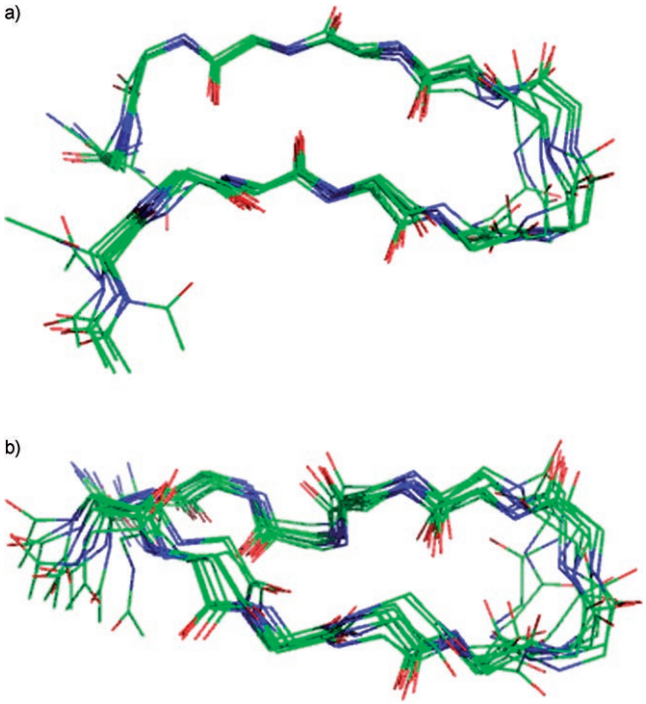

Figure 13. Backbones of superimposed NMR structures from simulated annealing runs. a) WKL and b) WKMe$_3$L.

bonding pattern expected for β-hairpin structure and the experimentally observed fraying at the termini (Figure 13a–b). The side-chain orientations in the average structure shown in Figure 14 also reflect what has been observed experimentally: orientation of the lysine side chain near the face of the tryptophan ring, with the ε-CH$_2$ packed into the ring, packing of the leucine with the tryptophan residue, and packing of the glutamic acid side chain against the lysine methylenes, with the carboxyl functionality directed away from the hydrophobic cluster. Unrestrained molecular dynamics simulations of these average structures in explicit water with the AMBER package indicates that these structures are stable over several nanoseconds of simulation time and are therefore not overly biased by the experimental restraints in our NMR structure calculations (Figure 15). The overall conclusion from the computational data is that 1) our initial hypothesis regarding the orientation of the lysine side chain with respect to the tryptophan is correct and 2) these hairpins contain a tightly packed hydrophobic cluster between residues in the non-hydrogen-bonding sites that is accurately described by both experimental and computational data.

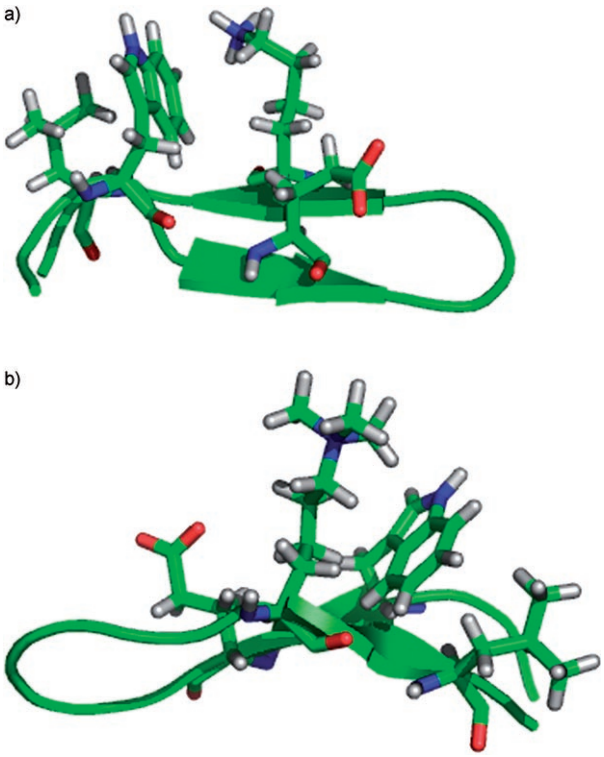

Figure 14. Averages of selected NMR structures from simulated annealing runs. a) WKL and b) $WKMe_3L$.

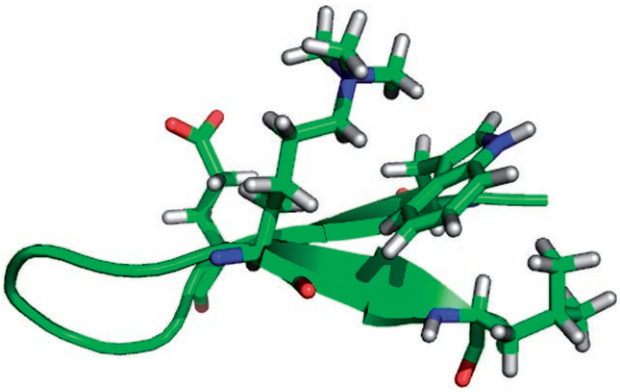

Figure 15. Low-energy structure of peptide $WKMe_3L$ from a two nanosecond MD simulation in AMBER.

Conclusion

The enhancement of the cation–π interaction by means of N-methylation within the context of a β-hairpin has been thoroughly investigated. Shortening the side chain decreases the magnitude of the observed interaction and substantially decreases hairpin stability. Other key factors of fold stability, including the formation of a hydrophobic cluster between Trp, Leu, Glu, and the methylated cationic side chain, have been shown to contribute substantially to the overall stability of the peptides studied. The incremental modulation of the thermodynamic profile of hairpin folding with increasing methylation reveals the contribution of each additional methyl group to the interaction and suggests a thermodynamic basis for discrimination between mono-, di-, and trimethylation in biological systems, as seen in the preferential binding of trimethylated lysines by PhD domains and chromodomains.[26] On a fundamental level, this study shows the ability of the Lys, Orn, and Dab side chains to maintain a favorable interaction with Trp, even as the geometry of the interaction appears to be changing. This is due in part to the flexibility of our β-hairpin model system, and due to the broad recognition surface of Trp, which makes it an easy target to hit. Furthermore, the examination of Orn and Dab residues versus Lys presents another means of stability control in designed proteins and receptors by the cation–π interaction. One can imagine the use of these three interactions to lend varying degrees of strength and specificity to designed systems. Studying these effects in a less solvent-exposed environment might lead to even better control of the interaction. Finally, this study highlights the interplay between β-sheet propensities, specific, and nonspecific hydrophobic interactions in determining the overall stability of β-hairpin model systems.

Experimental Section

Fmoc-monomethyl(*o*NBS)ornithine and Fmoc-monomethyl-(*o*NBS)diaminobutyric acid (4): Boc-ornithine-OH (0.358 g, 1.5 mmol) was taken up into NaOH (15 mL, 1 N) in a 100 mL round-bottomed flask and cooled in an ice bath. *o*-Nitrobenzenesulfonyl chloride (2.05 g, 9.25 mmol) was dissolved in diethyl ether (30 mL) and added dropwise over a ten-minute period with stirring to the chilled aqueous solution by means of a separatory funnel. After addition was complete, the two-phase solution was allowed to warm slowly to room temperature with vigorous stirring over 14 h. Next, the reaction mixture was transferred into a separatory funnel, and the aqueous and organic layers were separated. The aqueous layer was washed with ether (2×25 mL), and then chilled to 0 °C. Gradual addition of HCl (1 N) to pH 4 resulted in the formation of a white precipitate. The chilled aqueous mixture was extracted with several volumes of ethyl acetate (3×50 mL). The ethyl acetate was dried with $MgSO_4$ and the solvent removed in vacuo, yielding a clear oil (0.327 g). The oil was subsequently taken up in NaOH (1 N 10 mL) with stirring in a 100 mL round-bottomed flask. Dimethyl sulfate (1 mL) was added and the solution was allowed to stir for 3 h. The reaction was followed by TLC (CH_2Cl_2/MeOH 10:1). The resulting aqueous solution was chilled to 0 °C and carefully acidified to pH 4 with HCl (1 N), resulting in the formation of a white precipitate. The acidic mixture was extracted with several volumes of ethyl acetate, which was dried with $MgSO_4$ and evaporated in vacuo to give a yellowish oil, which was purified by means of silica-gel chromatography (CH_2Cl_2/MeOH 10:1) to give compound **3**. (Yield: 0.215 g, 0.5 mmol, 33 % yield). ^{1}H NMR (600 MHz, $CDCl_3$): δ = 7.93 (d, 1H), 7.66 (m, 2H), 7.57 (d, 1H), 5.25 (br s, 1H), 4.22 (m, 1H), 3.24 (m, 2H), 2.85 (s, 3H), 1.862 (m, 1H), 1.66 (m, 3H), 1.40 ppm (s, 9H); ESIMS: *m*/*z*: calcd for: 431.14; found: 431.2.

Compound **3** was taken up into a solution of trifluoroacetic acid (5 mL) in CH_2Cl_2 (15 mL) and stirred for 30 min to remove the Boc group. After removing the solvent in vacuo, the remaining residue was triturated with ether, resulting in a white solid. The material was extracted into water (10 mL), frozen, and lyophilized. The resulting compound was dissolved in THF (25 mL) and chilled to ice temperature. DIPEA was added (causing the compound to precipitate out of solution), followed by gradual addition of Fmoc-Cl in THF (20 mL). Upon completion of addition of Fmoc-Cl, the precipitated compound disappeared and the solution was removed from the ice bath and stirred for 10 h. Solvent removal in vacuo

produced a residue which was washed with several volumes of ether, and was then carefully decanted. The remaining residue was taken up into ethyl acetate (50 mL) and washed with water (2×10 mL). The resulting organic solution was dried with $MgSO_4$ and evaporated to dryness, resulting in a clear oil. Compound **4** was purified by means of silica-gel chromatography (column flushed with 100 mL CH_2Cl_2; product eluted with CH_2Cl_2/MeOH 10:1) to give a white solid (0.200 g, 0.362 mmol, 72% yield for two steps). ^{1}H NMR (600 MHz, $CDCl_3$): δ = 7.954 (d, 1H), 7.748 (d, 2H), 7.652 (m, 2H), 7.58 (m, 3H), 7.384 (dd, 2H), 7.299 (dd, 2H), 5.325 (d, 1H), 4.405 (s, 2H), 4.208 (t, 1H), 3.320 (m, 1H), 3.238 (m, 1H), 2.862 (s, 3H), 1.96 (m, 1H), 1.70 ppm (m, 3H); ESIMS: *m*/*z*: calcd for: 553.15; found: 553.2.

An identical procedure was followed for the synthesis of Fmoc-monomethyldiaminobutyric acid (*o*NBS), by using Boc-diaminobutyric acid (0.358 g, 1.64 mmol). The product was isolated as a clear oil (0.180 g, 0.334 mmol). ^{1}H NMR (600 MHz, $CDCl_3$): δ = 7.928 (d, 1H), 7.739 (d, 2H), 7.655 (m, 2H), 7.57 (m, 3H), 7.373 (dd, 2H), 7.30 (dd, 2H), 5.478 (d, 1H), 4.463 (s, 2H), 4.234 (t, 1H), 3.334 (m, 1H), 3.213 (m, 1H), 2.885 (s, 3H), 2.195 (m, 1H), 1.855 ppm (m, 1H); ESIMS: *m*/*z*: calcd for: 539.14; found: 539.2.

Fmoc-dimethyl ornithine and Fmoc-dimethyl diaminobutyric acid (6a): Boc-ornithine **1a** (0.175 g; 0.75 mmol) was taken up in MeOH (10 mL) in a 100 mL round-bottomed flask with stirring. Formaldehyde (340 μL, 37%, 11 mmol) was added to the solution, which was then allowed to stir for 5 min. The flask was flushed with N_2, followed by the addition of 0.33 g of 10% Pd/C. Next, the flask was plugged with a rubber septum and flushed with H_2 gas. A balloon of H_2 was attached, and the reaction stirred for 24 h. The contents of the flask were then filtered to remove the catalyst and the solvent removed in vacuo to give compound **5a**. The reaction was monitored by TLC (CH_2Cl_2/MeOH 5:1) with ninhydrin staining. Reaction completion was confirmed with RP-HPLC (C18 column; gradient of 5–60% CH_3CN in water over 30 min). ^{1}H NMR (600 MHz, $CDCl_3$): δ = 5.66 (s, 1H), 4.04 (s, 1H), 2.94 (m, 1H), 2.76 (m, 1H), 2.66 (s, 6H), 1.72–1.81 (m, 3H), 1.52–1.60 (m, 1H), 1.38 ppm (s, 9H); ESIMS: *m*/*z*: calcd for: 260.17; found: 260.2. Compound **5a** was taken up into a solution of trifluoroacetic acid (5 mL) and triisopropylsilane (250 mL) in CH_2Cl_2 (15 mL) and stirred for 30 min to remove the Boc group. After removing the solvent in vacuo, the remaining residue was triturated with ether, resulting in an oily precipitate. The material was extracted into water (10 mL), frozen, and lyophilized to dryness. The resulting oil was then dissolved in water (10 mL) and added to a 100 mL round-bottomed flask equipped with a stirbar. Sodium carbonate (2.3 mmol, 0.240 g) was added to the solution, followed by dioxane (5 mL). The resulting solution was stirred for 10 min at 0°C. Fmoc-OSu (0.825 mmol; 0.278 g) was dissolved in dioxane (5 mL) and added dropwise to the ice-cold solution over 10 min. The resulting mixture was stirred for 1 h at 0°C and 16 h at room temperature. The reaction was followed by TLC (CH_2Cl_2/MeOH 10:1, ninhydrin staining). The mixture was then washed with ether (2×25 mL) and acidified with HCl (1N) to pH 3. The acidic solution was extracted with ethyl acetate (4×50 mL), dried with sodium sulfate, and the solvent was removed in vacuo to give 0.252 g (0.659 mmol, 88% yield for two steps) of compound **6a** as an amorphous white solid. ^{1}H NMR (600 MHz, $CDCl_3$): δ = 7.710 (d, 2H), 7.559 (dd, 2H), 7.346 (dd, 2H), 7.252 (dd, 2H), 6.149 (d, 1H), 4.304 (m, 2H), 4.150 (t, 1H), 3.111 (m, 1H), 2.984 (m, 1H), 2.746 (s, 6H), 1.90–1.96 (m, 1H), 1.77–1.84 ppm (m, 3H); ESIMS: *m*/*z*: calcd for: 382.19; found: 382.3.

An identical procedure was followed for the synthesis of Fmoc-dimethyldiaminobutyric acid, by using Boc-diaminobutyric acid (0.164 g; 0.75 mmol), 30% formaldehyde (340 μL), Pd/C (0.033 g) in MeOH (10 mL), and H_2O (1 mL). ^{1}H NMR (600 MHz, $CDCl_3$): δ = 5.85 (s, 1H), 3.95 (s, 1H), 3.11 (m, 1H), 2.96 (m, 1H), 2.68 (s, 6H), 2.05–2.19 (m, 2H), 1.40 ppm (s, 9H). ESIMS: calcd: 246.16; found: 246.2. Deprotection with TFA and reprotection with Fmoc-OSu by an identical procedure gave 0.173 g of compound **7b** as a clear oil (0.47 mmol, 63% yield for two steps). ^{1}H NMR (600 MHz, $CDCl_3$): δ = 7.737 (d, 2H), 7.590 (m, 2H), 7.374 (dd, 2H), 7.289 (dd, 2H), 6.239 (s, 1H), 4.331 (m, 2H), 4.185 (t, 1H), 3.160 (m, 1H), 3.045 (m, 1H), 2.739 (s, 6H), 2.16–2.28 ppm (m, 2H); ESIMS: *m*/*z*: calcd for: 368.17; found: 368.2.

Trimethylated lysine, ornithine, and diaminobutyric acid: Trimethylated amino acids were synthesized by following the procedure of Kretsinger and Schneider.[11] The peptides were synthesized by using Fmoc-Lys(Me)$_2$-OH purchased from either Anaspec, Bachem, Fmoc-Orn(Me)$_2$-OH or Fmoc-Dab(Me)$_2$-OH synthesized by methods described above. The dimethylated amino acid-containing peptides (0.100 mmol scale) were reacted prior to cleavage from the resin with MTBD (18 μL, 0.125 mmol) and methyl iodide (62 μL, 1 mmol) in DMF (5 mL) for 4 h with bubbling N_2 in a peptide synthesis flask stoppered with a vented septum. After washing the resin with DMF (3×), CH_2Cl_2 (3×), and drying, the peptide was cleaved with a cocktail of 90% TFA/5% Triisopropylsilane/5% H_2O for 3 h. The peptide was then purified by standard HPLC methods.

Peptide synthesis and purification: Peptide synthesis was performed on an Applied Biosystems Pioneer peptide synthesizer by using standard FMOC solid-phase peptide synthesis methodology. Non-commercially available amino acids were in some cases coupled by hand. Peptides were purified with reverse-phase HPLC, lyophilized, and characterized by MALDI or ESI-TOF mass and NMR spectroscopy.

NMR spectroscopy: NMR samples were made in concentrations of approximately 1 mM and analyzed on a Varian Inova 600 MHz spectrometer. Samples were dissolved in D_2O buffered to pD 4.0 (uncorrected) with 50 mM [D_3]NaOAc, unless otherwise noted. Amine and amide resonances were assigned in 60% H_2O solutions. ^{1}D NMR spectra were collected by using 32 K data points and between 8 and 64 scans by using a 1–3 s presaturation. All ^{2}D NMR experiments used pulse sequences from the Chempack software including TOCSY, DQCOSY, gCOSY, and NOESY. ^{2}D NMR scans were taken with 16–64 scans in the first dimension and 64–256 scans in the 2nd dimension. All spectra were analyzed by using standard window functions (Sinebell and Gaussian). Mixing times of 0.5 or 0.6 s were used in the NOESY spectra. Assignments were made by using standard methods as described by Wüthrich.[27] Temperature calibrations were made by using MeOH and ethylene glycol standards.

pH studies: Three buffer solutions in D_2O were used to analyze the sensitivity of peptide stability to changes in pH: pH 7.4 (10 mM sodium phosphate buffer), pH 4 (50 mM sodium acetate buffer), and pH 1.10 (phosphoric acid buffer). pH values uncorrected for deuterium isotope effects.

NMR structure calculation and MD simulation: NOEs were classified as strong, medium, or weak by visual inspection. Accordingly, upper bounds for distance restraints were set at 5.0, 3.5, or 2.5 Å.[28] NMR structures were calculated by using a simulated annealing protocol within the program CNS Solve.[25] Hydrogen bonds were enforced with upper limits of 2.0 Å and assigned based on backbone amide shifts (see the Supporting Information). In the calculation of WKL, 23 nonsequential NOEs were used and 34 nonsequential NOEs were used in the calculation of the structure of WKMe$_3$L. All available backbone amide, H_α, and side-chain ^{1}H chemical shifts were also employed in the calculations by a harmonic potential with a primary chemical shift force value of 10 (61 observed chemical shifts; random coil values taken from 7 mers). Two rounds of simulated annealing were employed in each calculation. In the first, 200 structures were generated from an extended starting structure. In the second, 50 structures were generated starting from an averaged folded structure taken from the initial run. The best structures were selected from the second run based on total energy and visual inspection and averaged. The average structures were subjected to an additional unconstrained conjugate gradient minimization.

The resulting average structure for WKMe$_3$L was used as the starting structure for an MD run in explicit water in AMBER.[29] Non-natural residues were constructed in xLeap and parameterized based on existing residues with scaled RESP charges (included in the Supporting Information). The starting structure was solvated in an octahedral box by using TIP3P water and the system charge neutralized with two chloride ions. The solvated system was minimized and then equilibrated by heating from 0 to 300 K over 20 ps. Finally, production MD were run at 300 K by using PME electrostatics and periodic boundary conditions within

Amber ff99. The lowest-energy structure was selected from the 2 ns run for demonstrative purposes. Additional simulation parameters and run data are given in the Supporting Information.

Acknowledgements

MLW gratefully acknowledges an Alfred P. Sloan foundation fellowship. RMH gratefully acknowledges support from a Burroughs Wellcome foundation fellowship and an ACS Division of Organic Chemistry fellowship. This work was funded by a grant from the NIH NIGMS (GM 071589).

[1] a) J. C. Ma, D. A. Dougherty, *Chem. Rev.* **1997**, *97*, 1303–1324; b) J. P. Gallivan, D. A. Dougherty, *Proc. Natl. Acad. Sci. USA* **1999**, *96*, 9459–9464.
[2] P. B. Crowley, A. Golovin, *Proteins Struct. Funct. Bioinf.* **2005**, *59*, 231–239.
[3] Q. Dai, C. Tommos, E. J. Fuentes, M. R. A. Blomberg, P. L. Dutton, A. J. Wand, *J. Am. Chem. Soc.* **2002**, *124*, 10952–10953.
[4] a) A. M. Lindroth, D. Shultis, Z. Jasencakova, J. Fuchs, L. Johnson, D. Schubert, D. Patnaik, S. Pradhan, J. Goodrich, I. Schubert, T. Jenuwein, S. Khorasanizadeh, S. E. Jacobsen, *Embo. J.* **2004**, *23*, 4286–4296; b) S. Khorasanizadeh, *Biophys. J.* **2003**, *84*, 485 A; c) S. Jacobs, J. Harp, S. Khorasanizadeh, *Biophys. J.* **2003**, *84*, 503 A; d) W. Fischle, Y. M. Wang, S. A. Jacobs, Y. C. Kim, C. D. Allis, S. Khorasanizadeh, *Genes Dev.* **2003**, *17*, 1870–1881; e) S. A. Jacobs, S. Khorasanizadeh, *Science* **2002**, *295*, 2080–2083.
[5] a) K. Scharer, M. Morgenthaler, R. Paulini, U. Obst-Sander, D. W. Banner, D. Schlatter, J. Benz, M. Stihle, F. Diederich, *Angew. Chem.* **2005**, *117*, 4474–4479; *Angew. Chem. Int. Ed.* **2005**, *44*, 4400–4404; b) P. C. Kearney, L. S. Mizoue, R. A. Kumpf, J. E. Forman, A. E. McCurdy, D. A. Dougherty, *J. Am. Chem. Soc.* **1993**, *115*, 9907–9919; c) A. McCurdy, D. A. Dougherty, *J. Am. Chem. Soc.* **1992**, *114*, 10314–10321.
[6] R. M. Hughes, M. L. Waters, *J. Am. Chem. Soc.* **2005**, *127*, 6518–6519.
[7] a) C. E. Stotz, E. M. Topp, *J. Pharm. Sci.* **2004**, *93*, 2881–2894; b) S. H. Gellman, *Curr. Opin. Chem. Biol.* **1998**, *2*, 717–725; c) M. Ramirez-Alvarado, T. Kortemme, F. J. Blanco, L. Serrano, *Bioorg. Med. Chem.* **1999**, *7*, 93–103.
[8] a) C. D. Tatko, M. L. Waters, *Protein Sci.* **2003**, *12*, 2443–2452; b) C. D. Tatko, M. L. Waters, *J. Am. Chem. Soc.* **2004**, *126*, 2028–2034.
[9] S. C. Miller, T. S. Scanlan, *J. Am. Chem. Soc.* **1997**, *119*, 2301–2302.
[10] a) L. Benoiton, *Can. J. Chem.* **1964**, *42*, 2043; b) J. Lamar, J. Hu, A. B. Bueno, H. C. Yang, D. Guo, J. D. Copp, J. McGee, B. Gitter, D. Timm, P. May, J. McCarthy, S. H. Chen, *Bioorg. Med. Chem. Lett.* **2004**, *14*, 239–243.
[11] J. K. Kretsinger, J. P. Schneider, *J. Am. Chem. Soc.* **2003**, *125*, 7907–7913.
[12] S. R. Griffith-Jones, A. J. Maynard, M. S. Searle, *J. Mol. Biol.* **1999**, *292*, 1051–1069.
[13] H. Guo, M. Karplus, *J. Phys. Chem.* **1994**, *98*, 7104–7105.
[14] A. J. Maynard, G. J. Sharman, M. S. Searle, *J. Am. Chem. Soc.* **1998**, *120*, 1996–2007.
[15] C. A. Hunter, S. Tomas, *Chem. Biol.* **2003**, *10*, 1023–1032.
[16] J. P. Gallivan, D. A. Dougherty, *Proc. Natl. Acad. Sci. USA* **1999**, *96*, 9459–9464.
[17] a) M. Stauffer, D. A. Dougherty, *Tetrahedron Lett.* **1988**, *29*, 6039; b) M. Stauffer, D. A. Dougherty, *Science* **1990**, *250*, 1558.
[18] A. W. Smith, H. S. Chung, Z. Ganim, A. J. Tokmakoff, *J. Phys. Chem. B* **2005**, *109*, 17025–17027.
[19] A. G. Cochran, N. J. Skelton, M. A. Starovasnik, *Proc. Nat. Acad. Sci.* **2001**, *98*, 5578–5583.
[20] V. V. Loladze, D. N. Ermolenko, G. I. Makhatadze, *Protein Sci.* **2001**, *10*, 1343–1352.
[21] MacSpartan 2004 (Wavefunction).
[22] a) A. G. Cochran, R. T. Tong, M. A. Starovasnik, E. J. Park, R. S. McDowell, J. E. Theaker, N. J. Skelton, *J. Am. Chem. Soc.* **2001**, *123*, 625–632; b) S. J. Russell, T. Blandl, N. Skelton, A. G. Cochran, *J. Am. Chem. Soc.* **2003**, *125*, 388–395.
[23] B. Ciani; M. Jordan, M. S. Searle, *J. Am. Chem. Soc.* **2003**, *125*, 9038–9047.
[24] K. Tsou, C. D. Tatko, M. L. Waters, *J. Am. Chem. Soc.* **2002**, *124*, 14917–14921.
[25] A. T. Brunger, P. D. Adams, G. M. Clore, W. L. Delano, P. Gros, R. W. Grosse-Kunstleve, J. S. Jiang, J. Kuszewski, N. Nilges, N. S. Pannu, R. J. Read, L. M. Rice, T. Simondson, G. L. Warren, *Acta Crystallogr. D* **1998**, *54*, 905–921.
[26] a) J. Wysocka, T. Swigut, H. Xiao, T. A. Milne, S. Y. Kwon, J. Landry, M. Kauer, A. J. Tackett, B. T. Chait, P. Badenhorst, C. Wu, C. D. Allis, *Nature* **2006**, *442*, 86–90; b) H. T. Li, S. Ilin, W. K. Wang, E. M. Duncan, J. Wysocka, C. D. Allis, D. J. Patel, *Nature* **2006**, *442*, 91–95; c) X. B. Shi, T. Hong, K. L. Walter, M. Ewalt, E. Michishita, T. Hung, D. Carney, P. Pena, F. Lan, M. R. Kaadige, N. Lacoste, C. Cayrou, F. Davrazou, A. Saha, B. R. Cairns, D. E. Ayer, T. G. Kutateladze, Y. Shi, J. Cote, K. F. Chua, O. Gozani, *Nature* **2006**, *442*, 96–99.
[27] K. Wüthrich, *NMR of Proteins and Nucleic Acids*, Wiley, **1986**.
[28] R. Mahalakshmi, S. Raghothama, P. J. Balaram, *J. Am. Chem. Soc.* **2006**, *128*, 1125–1138.
[29] D. A. Case, T. A. Darden, T. E. Cheatham, III, C. L. Simmerling, J. Wang, R. E. Duke, R. Luo, K. M. Merz, B. Wang, D. A. Pearlman, M. Crowley, S. Brozell, V. Tsui, H. Gohlke, J. Mongan, V. Hornak, G. Cui, P. Beroza, C. Schafmeister, J. W. Caldwell, W. S. Ross, P. A. Kollman (**2004**), AMBER 8, University of California, San Francisco.

Received: December 6, 2006
Published online: April 12, 2007

